Inundation Extent Mapping Using Dual-Polarimetric Sentinel-1 SAR Data

Woohyun Jeon (1), Jonghyuk Yi (1), Youseung Kim (1)

[1] SELAB, Inc., 8 Nonhyeon-ro 150-gil, Gangnam-gu, Seoul, 06049, Korea
Email: whjeon@selab.co.kr; yi@selab.co.kr; yskim@selab.co.kr

KEY WORDS: flood inundation mapping, Sentinel-1, synthetic aperture radar (SAR), dual-polarization

ABSTRACT: Given the growing threats of extreme precipitation events, there exists a strong demand for inundation mapping in near real-time (NRT) for further operational response. In this context, synthetic aperture radar (SAR) data provides valuable information due to cloud penetration capability of microwave. In this regard, Sentinel-1 imagery, with the short revisit time of six days, give an unprecedented opportunity to generate multitemporal datasets, allowing change detection approach. Furthermore, dual-polarized information can be acquired, enabling more informative analysis. Considering above issues, this study proposes the complementary use of interferometric coherence and intensity values. The proposed framework is based on two step-approach that first step consists of exploiting coherence and intensity of multitemporal Sentinel-1 data, followed by change detection. The data processing was conducted using the off-the-shelf ENVI/SARscape5.5 software. Results show that flood-prone areas can be highlighted with more accurate identification of the inundated areas. Hence, it can be concluded that this study contributes to demonstrating the potentiality of dual-polarized Sentinel-1 data for urban inundation extent mapping.

1. Introduction

Floods are one of the most frequent natural disasters, resulting in high socio-economic impacts. Given that growing threats of extreme precipitation events due to recent climate change, near-real-time (NRT) inundation mapping during flood events plays an essential role to support further operational responses to mitigate losses (Cian, Marconcini, and Ceccato, 2015). This issue is of great importance in Indonesia, where has an annual monsoon season and geographic features, resulted in certain flood-prone areas (Chung et al., 2016). Further, along with economics growth in Indonesia, flood vulnerability has become growing concern. Hence, it is vital to monitor inundated areas during monsoon periods, further contributing to flood event management with preventing unprecedented crisis.

Since flood conditions often occur with harsh weather conditions, optical data are infeasible to map inundated areas during floods (Uddin, Matin, and Meyer, 2019). Regarding the penetration capability of microwave, synthetic aperture radar (SAR) systems have proven to be an effective tool over optical systems (Giustarini et al. 2014; Twele et al., 2016). Considerable SAR techniques have focused on developing algorithms for delineating inundated areas. The most common technique is based on the change detection (CD), analyzing a set of images acquired pre- and post- flood events (Gong et al., 2014; Lu et al., 2014; Lu et al., 2015; Pradhan, Sameen, and Kalantar, 2017). A representative benefit of CD techniques to mask out the permanent water bodies and some water look-alike objects (Li et al., 2018).

Generally, SAR intensity (i.e., the backscattering coefficient σ^0) is considered as a primary indicator for detecting inundated areas (Martinis and Rieke, 2015). The principle is to detect the change of scattering mechanism resulted from flooding event, leading to discriminate flooded and non-flooded areas. However, considering urban and agricultural areas with surface and vertical structures, SAR intensity is not sufficient to detect enhancement of double bounce effect resulting from the presence of floodwater (Mason et al., 2014). In that, recent studies have proven the interferometric coherence (γ) as an attractive alternative (Pulvirenti et al., 2016; Refice et al., 2014). Note that data acquisition with short temporal baseline has highly recommended for the coherence analysis.

Following the launch of Sentinel-1 satellites with a repeat period of six days, timely data can be

acquired, leading to an unprecedented opportunity for dynamic inundation mapping. Indeed, it is worth noting that dual-polarized channels can be acquired, offering possibilities for more accurate identification of inundated areas. In this regard, the objective of this study is to propose the complementary use of interferometric coherence and intensity values of dual-polarized Sentinel-1 dataset. Further, this study demonstrates the feasibility of Sentinel-1 data for NRT inundation mapping. The remaining of this paper is organized as follows. Section 2 introduces the study area, dataset, and methodology. Then, Section 3 provides the results and discussion, followed by presenting conclusion in Section 4.

2. Methodology

2.1 Study area and dataset

A heavy rainfall was struck the Papua province of Indonesia, resulting devastating flash flood on 16 March 2019. Landslides and floods have occurred across the Jayapura regency, causing severe losses of human and infrastructure. Indeed, Jayapura administration officials have declared 14-day emergency beginning from 16 March 2019. Therefore, NRT inundation mapping near the Jayapura regency is essential for period of emergency in order to support the operational response. Study area is illustrated on Figure 1, with pre-event Sentinel-1 intensity image.

Figure 1. Study area.

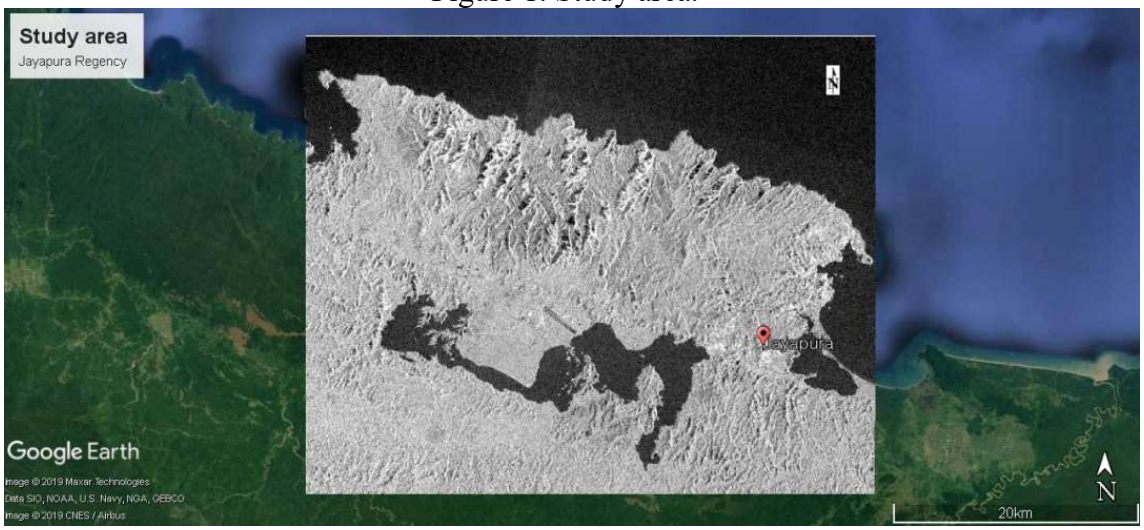

In this study, Sentinel-1 data as single look complex (SLC) products with interferometric wide (IW) mode were acquired across the study area. Both co-polarized (vertical transmit and vertical receive (VV)) and cross-polarized (vertical transmit and horizontal receive (VH)) channels were used. Indeed, pre- and post-flood datasets were selected to obtain multi-temporal analysis. The detailed characteristics of datasets are provided in Table 1.

Table 1. Detailed characteristics of datasets.

Sensor	Acquisition Date	Polarization	Path Direction	$B_{\perp}$ (m)	B_T (days)
Sentinel-1	2019/02/24			-34.94	12
Level1	2019/03/08	VV/VH	Descending	0	0
SLC data	2019/03/20			-46.96	12

2.2 SAR data processing

The methods used in this study are illustrated in Figure 2. The procedure is divided into two main steps: backscattering coefficient and interferometric coherence analysis. All the processing were conducted on the off-the-shelf ENVI/SARscape5.5 software.

Figure 2. Flowchart of this study.

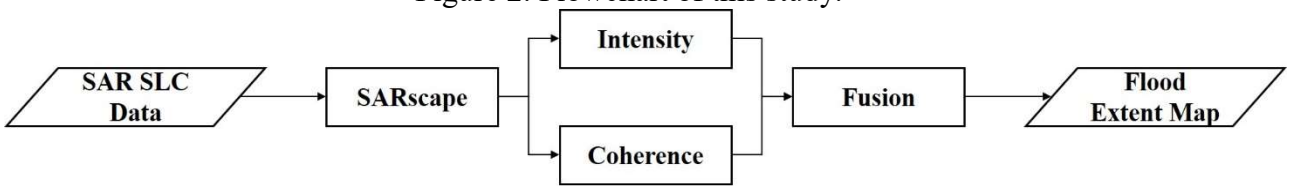

The intensity values of Sentinel-1 data were converted into backscattering coefficients. Multi-looking and speckle filtering were adopted to reduce the effect of speckle noise. Besides, co-registration and geocoding were conducted with 1 arc-sec digital elevation model (DEM) of the Shuttle Radar Topography Mission (SRTM) data. Figure 3 shows pre- and post-event Sentinel-1 intensity images of VV and VH polarizations.

Figure 3. Pre- and post-event Sentinel-1 intensity images.

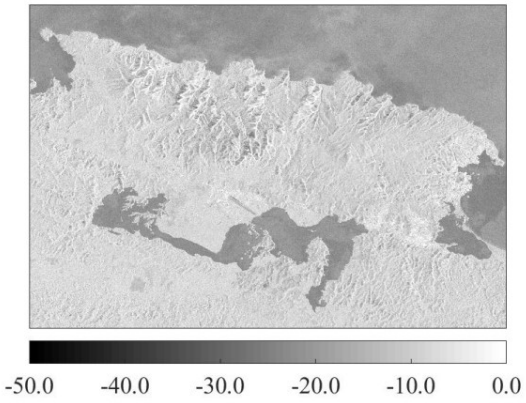

(a) Pre-event / VV polarization

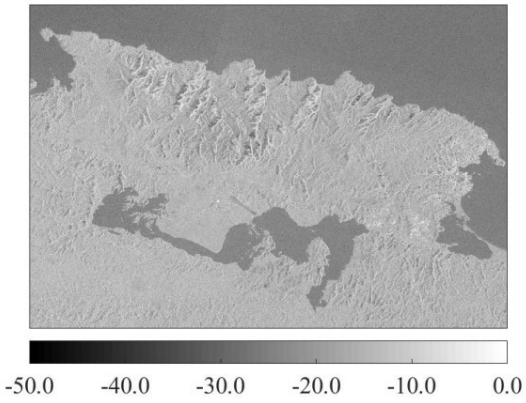

(b) Pre-event / VH polarization

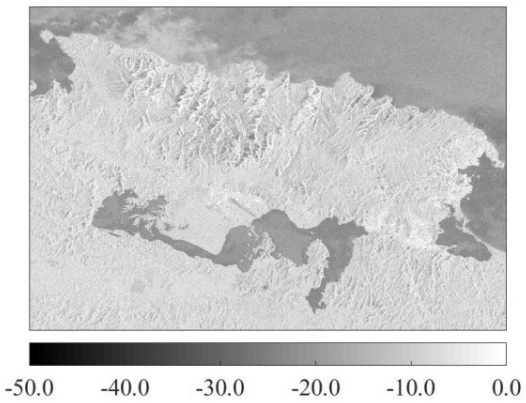

(c) Post-event / VV polarization

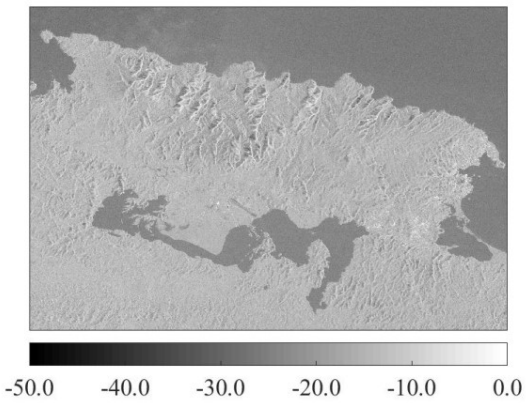

(d) Post-event / VH polarization

Further, change detection approach was adopted by simple differencing between pre- and post-event images (Equation 1, i denotes polarization (VV, VH)). In order to conjugative use with coherence results, normalization was conducted on the difference image (Equation 2). Besides, in order to verify the informative analysis of dual-polarization data, linear combination was adopted for simplicity (Equation 3). In this study, coefficients are determined proportional to the mean value of each CD results, assuming that higher values indicate more sensitive to the presence of flooding.

$$d_i = \left|\sigma^0_{pre-event,i} - \sigma^0_{post-event,i}\right| \tag{1}$$

$$\widehat{d_i} = \frac{d_i - min(d_i)}{\max(d_i) - \min(d_i)} \tag{2}$$

$$d = \sum \alpha_i \cdot \hat{d}_i \tag{3}$$

Additionally, interferometric coherence was derived from Sentinel-1 data. Similar as the above method, change detection results were extracted after simple differencing and normalization (Equation 4, 5, 6). Figure 4 shows the interferometric coherence value of pre- and post-event Sentienl-1 images.

$$c_i = \gamma_{co-event,i} - \gamma_{pre-event,i} \tag{4}$$

$$\hat{c}_i = \frac{c_i - min(c_i)}{\max(c_i) - \min(c_i)} \tag{5}$$

$$c = \sum \beta_i \cdot \hat{c}_i \tag{6}$$

Figure 4. Pre- and co-event Sentinel-1 coherence images.

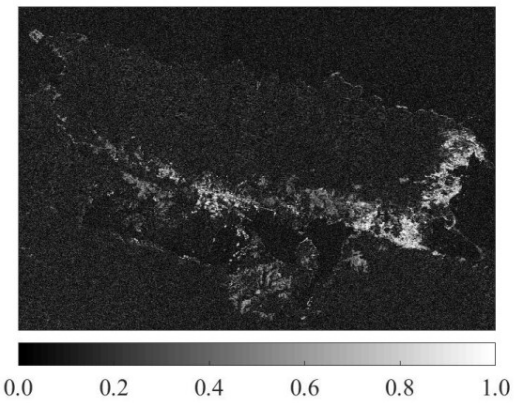

(a) Pre-event / VV polarization

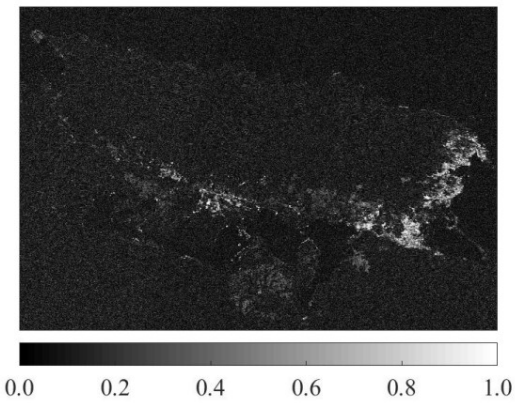

(b) Pre-event / VH polarization

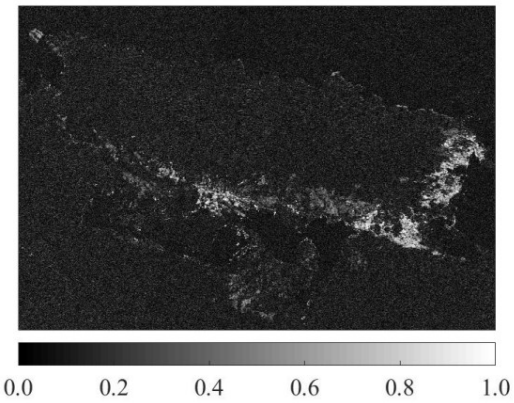

(c) Co-event / VV polarization

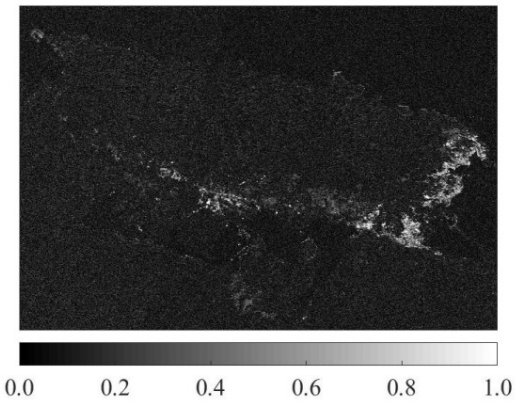

(d) Co-event / VH polarization

Final flood extent map was generated by fusing the change detection results from backscattering coefficient and coherence. Indeed, coefficients (γ and δ) was determined after conducting histogram matching with intensity (c) and coherence (d) results (Equation 7).

$$z = \gamma \cdot c + \delta \cdot d \tag{7}$$

3. Results and Discussion

Figure 5 shows the intensity and coherence CD results on each polarization. Among intensity results, some false alarms can be observed, indicating rough surface of the sea due to the harsh weather conditions. Further, among coherence results, both results show similar distribution, however, it can be seen that more distinct high values can be observed on the VV polarization results. Considering intensity CD results from VH polarization, there is a remarkable agreement with coherence CD results. These alarms are possibly a result of building collapse, leading to an increase of volume scattering mechanism (Twele et al., 2016).

Figure 5. Change detection results.

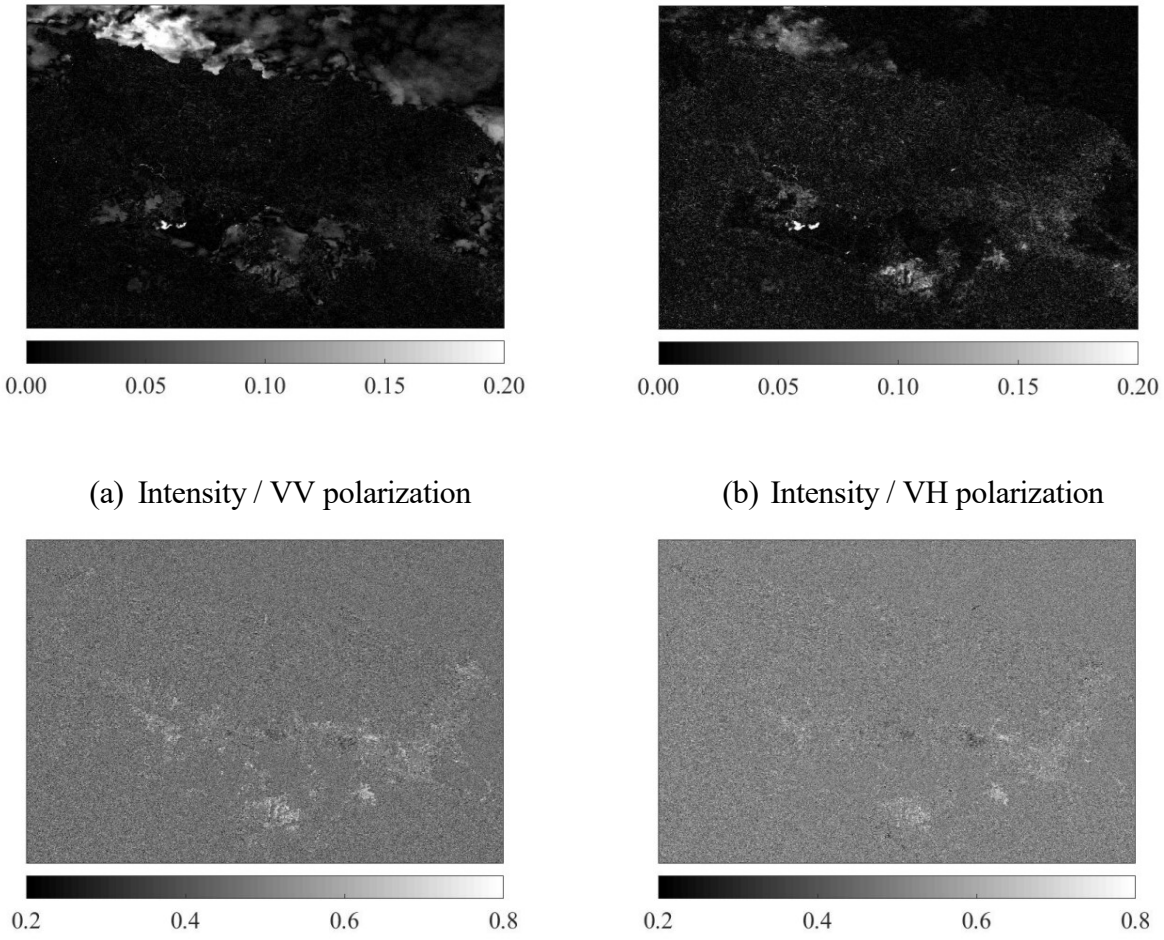

(a) Intensity / VV polarization

(b) Intensity / VH polarization

(c) Coherence / VV polarization

(d) Coherence / VH polarization

For further comparative analysis, Figure 6 illustrates CD results from intensity, coherence, and fusion. It can be verified that CD results from intensity and coherence show some different distribution. The reason is that high coherence value indicates the collapse of the buildings due to the landslides, while intensity indicates change of the scattering mechanism due to the presence of flooded water. Consequently, by fusing both results, flood-prone areas can be highlighted with more accurate identification of the inundated areas.

Figure 6. Change detection results.

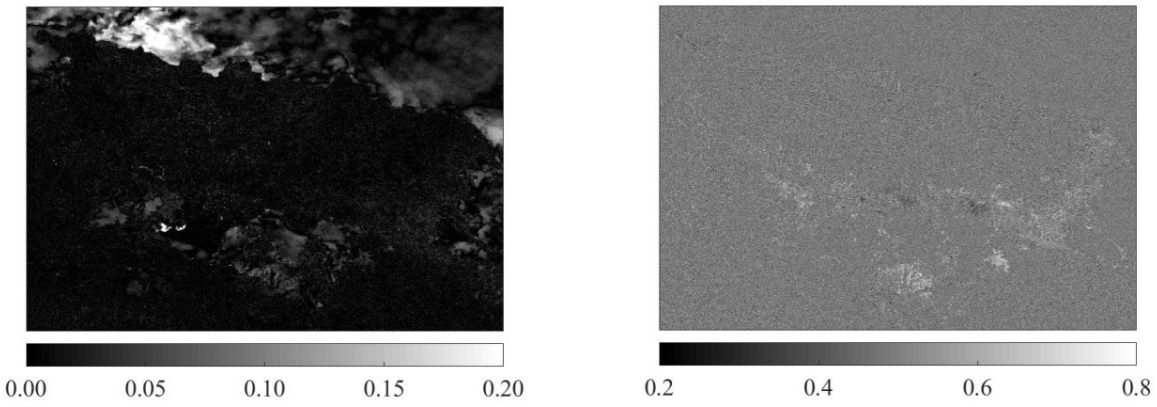

(a) Intensity (b) Coherence

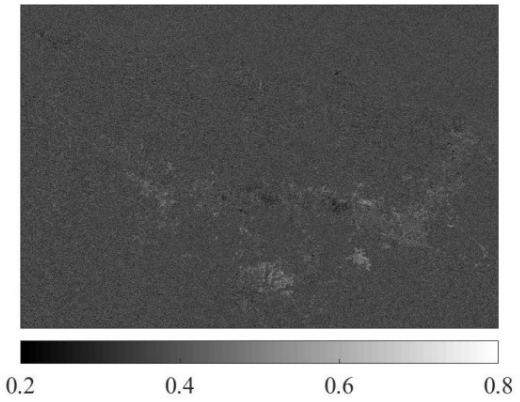

(c) Fusion

4. Conclusions

In this study, an analysis of multi-temporal Sentinel-1 SAR datasets was performed to identify inundated areas by investigating the change of backscattering coefficient and coherence values. The focus is on the Jayapura regency where devastated landslides and floods have affected. Experimental results have demonstrated that complementary use of intensity and coherence value leads to the more accurate detection of inundated areas. Further studies would validate the results and compare the state-of-the-art inundation mapping algorithms.

Acknowledgment

This work was supported by Korea Environment Industry & Technology Institute (KEITI) through Water Management Research Program, funded by Korea Ministry of Environment (MOE) (79620).

References

Chung, H. W., Liu, C. C., Cheng, I. F., Lee, Y. R., and Shieh, M. C., 2015. Rapid response to a typhoon-induced flood with an SAR-derived map of inundated areas: case study and validation. Remote Sensing, 7 (9), pp. 11954-11973.

Cian, F., Marconcini, M., and Ceccato, P., 2018. Normalized difference flood index for rapid flood mapping: Taking advantage of EO big data. Remote Sensing of Environment, 209, pp. 712-730.

Giustarini, L., Hostache, R., Matgen, P., Schumann, G. J. P., Bates, P. D., and Mason, D. C., 2012.

A change detection approach to flood mapping in urban areas using TerraSAR-X. IEEE Transactions on Geoscience and Remote Sensing, 51 (4), pp. 2417-2430.

Gong, M., Li, Y., Jiao, L., Jia, M., and Su, L., 2014. SAR change detection based on intensity and texture changes. ISPRS Journal of Photogrammetry and Remote Sensing, 93, pp. 123-135.

Li, Y., Martinis, S., Plank, S., and Ludwig, R., 2018. An automatic change detection approach for rapid flood mapping in Sentinel-1 SAR data. International Journal of Applied Earth Observation and Geoinformation, 73, pp. 123-135.

Lu, J., Li, J., Chen, G., Zhao, L., Xiong, B., and Kuang, G., 2015. Improving pixel-based change detection accuracy using an object-based approach in multitemporal SAR flood images. IEEE Journal of Selected Topics in Applied Earth Observations and Remote Sensing, 8 (7), pp. 3486-3496.

Lu, J., Giustarini, L., Xiong, B., Zhao, L., Jiang, Y., and Kuang, G., 2014. Automated flood detection with improved robustness and efficiency using multi-temporal SAR data. Remote Sensing Letters, 5 (3), pp. 240-248.

Martinis, S., and Rieke, C., 2015. Backscatter analysis using multi-temporal and multi-frequency SAR data in the context of flood mapping at River Saale, Germany, Remote Sensing, 7 (6), pp. 7732-7752.

Mason, D. C., Glustarini, L., Garcia-Pintado, J., and Cloke, H. L., 2014. Detection of flooded urban areas in high resolution synthetic aperture radar images using double scattering, International Journal of Applied Earth Observation and Geoinformation, 28, pp. 150-159.

Pradhan, B., Sameen, M. I., and Kalantar, B., 2017. Optimized rule-based flood mapping technique using multitemporal RADARSAT-2 images in the tropical region. IEEE Journal of Selected Topics in Applied Earth Observations and Remote Sensing, 10 (7), pp. 3190-3199.

Pulvirenti, L., Chini, M., Pierdicca, N., and Boni, G., 2016. Use of SAR data for detecting floodwater in urban and agricultural areas: the role of the interferometric coherence. IEEE Transactions on Geoscience and Remote Sensing, 54 (3), pp. 1532-1544.

Refice, A., Capolongo, D., Pasquariello, G., D'Addabbo, A., Bovenga, F., Nutricato, R., …, and Pietranera, L., 2014. SAR and InSAR for flood monitoring: examples with COSMO-SkyMed data. IEEE Journal of Selected Topics in Applied Earth Observations and Remote Sensing, 7 (7), pp. 2711-2722.

Twele, A., Cao, W., Plank, S., and Martinis, S., 2016. Sentinel-1-based flood mapping: a fully automated processing chain. International Journal of Remote Sensing, 37 (13), pp. 2990-3004.

Uddin, K., Matin, M. A., and Meyer, F. J., 2019. Operational flood mapping using multi-temporal Sentinel-1 SAR images: a case study from Bangladesh, Remote Sensing, 11, 1581.